Deformable Tissue Parameterized by Properties of Real Biological Tissue

Anderson Maciel, Ronan Boulic, and Daniel Thalmann

Virtual Reality Lab, École Polytechnique Fédérale de Lausanne,
CH 1015 Lausanne, Switzerland
{anderson.maciel, ronan.boulic, daniel.thalmann}@epfl.ch
http://vrlab.epfl.ch

Abstract. Realistic mechanical models of biological soft tissues are a key issue to allow the implementation of reliable systems to aid on orthopedic diagnosis and surgery planning. We are working to develop a computerized soft tissues model for bio-tissues based on a mass-spring-like approach. In this work we present several experiments towards the parameterization of our model from the elastic properties of real materials.

1 Introduction

Biomechanics literature provides a number of mathematical models that approximate the behavior of bio-tissues and bio-structures. Most of them are typically conceptual. They are used in Biomechanics to understand the complex behavior of materials that are heterogeneous, anisotropic, viscoelastic, and which properties may drastically change due to environmental and use conditions. However, to be applied on graphical computer simulation of biomechanical systems like the musculoskeletal system, existent models have to be converted and simplified.

We are currently working on a generalized approach towards functional modeling of human articulations. We plan to use such articulation model in medical applications to aid on diagnosis of joint disease and planning of surgical interventions. Our approach is based on a biomechanical model of the tissues present in the joint. This model relies on the mechanical and physical properties of biomaterials to provide correct motion, contact and deformation. The present work, that is a continuation of [1], presents part of our biomechanical model. It deals with the important issue of representing the mechanical properties of real biological soft tissues in their virtual models.

1.1 Objectives

A number of computational methods to simulate soft tissues have been proposed. In this work we use a generalized mass-spring model, called molecular model [2], to simulate the behavior of cartilage and ligament. However, though mass-spring is a

classical deformation approach, to set up the parameters of the model is not trivial. This problem is still more intricate if the behavior of a complex real material is intended to be represented.

The main goal of this work, thus, is to find a configuration of the elasticity coefficients of all springs in our molecular system, such that the elasticity of the whole piece of virtual tissue corresponds to the elasticity of the material it is supposed to be made of. It is important to say that we are mostly interested now in the elastic part of the material behavior. Non-linear parts of the stress-strain curve are out of the scope of the present paper.

1.2 Contents

Section 2 brings an overview of bio-tissues properties, particularly tissues of joints. Next, in section 3, we present the computational models most widely applied to soft tissues modeling. Following in the same chapter, the molecular system we are developing is introduced and the issues related to the goal of this work are discussed. Section 4 brings our implementation of the model and a collection of comparative tests performed on the top of it. Finally, our conclusions and future directions are rendered in the section 5.

2 Bio-tissues Properties

The composition and behavior of bones, cartilages and ligaments has been studied for many years. However, though we know much about these tissues, newer and better measurement techniques continuously update the available data. In this section, a brief presentation of the material properties of the main tissues involved in a joint is done. Muscles and tissues of superior layers will not be discussed here because of their active role (muscles produce force) and their less significant influence on the joint range of motion. So, let us see the properties of bone, cartilage and ligament.

2.1 Bone

Bone is identified as either cancellous (also referred to as trabecular or spongy) or cortical (also referred to as compact) [3, 4], see Fig. 1. The basic material comprising cancellous and compact bone appear identical, thus the distinction between the two is the degree of porosity and the organization. The porosity of cortical bone ranges from 5 to 30% while cancellous bone porosity ranges from 30 to 90%. Bone porosity is not fixed and can change in response to altered loading, disease, and aging.

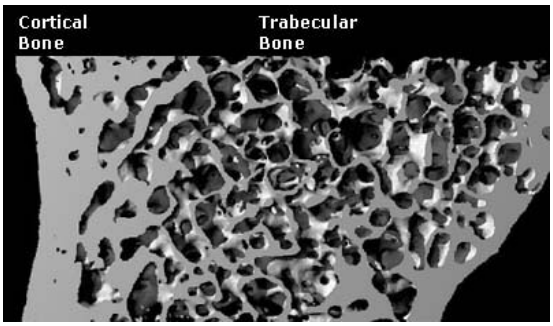

Fig. 1. Bone structure with its different layers. (Photograph by Dr. Yebin Jiang [5])

Cancellous bone is actually extremely anisotropic and inhomogeneous. Cortical bone, on the other hand, is approximately linear elastic, transversely isotropic and relatively homogenous. The material properties of bone are generally determined using mechanical testing procedures; however, ultrasonic techniques have also been employed. Force-deformation (structural properties) or stress-strain (material properties) curves can be determined by means of such tests. Bone shows a linear range in which the stress increases in proportion to the strain. The slope of this region is defined as Young's Modulus or the Elastic Modulus. However, the properties of bone and most biological tissues depend on the freshness of the tissue. These properties can change within a matter of minutes if allowed to dry out. Cortical bone, for example, has an ultimate strain of around 1.2% when wet and about 0.4% if the water content is not maintained.

2.2 Cartilage

Articular cartilage, also called hyaline cartilage, is made of a multiphasic material with two major phases: a fluid phase composed by water (68-85%) and electrolytes, and a solid phase composed by collagen fibrils (primarily type II collagen) (10-20%), proteoglycans and other glycoproteins (5-10%), and the chondrocytes (cartilaginous cells) [6]. The cartilaginous tissue is extremely well adapted to glide. Its coefficient of friction is several times smaller than the one between the ice and an ice skate. There are electrostatic attractions between the positive charges along the collagen molecules and the negative charges that exist along the proteoglycan molecules. Hydrostatic forces also exist as forces are applied to cartilage and the fluid tries to move throughout the tissue. It is the combined effect of all these interactions that give rise to the mechanical properties of the material.

Like bone, the properties of cartilage are anisotropic. The anisotropy results in part from the structural variations. Because of its structure, cartilage is rather porous, allowing fluid to move in and out of the tissue. When the tissue is subjected to a compressive stress, fluid flows out of the tissue. Fluid returns when the stress is removed. The mechanical properties of cartilage change with its fluid content, thus making it important to know the stress-strain history of the tissue to predict its load carrying capacity. The material properties also change with pathology. The compressive aggre-

gate modulus for human articular cartilage correlates in an inverse manner with the water content and in a direct manner with proteoglycan content per wet weight. There is no correlation with the collagen content thus suggesting that proteoglycans are responsible for the tissue's compressive stiffness. See Fig. 2 for elastic behavior of cartilage.

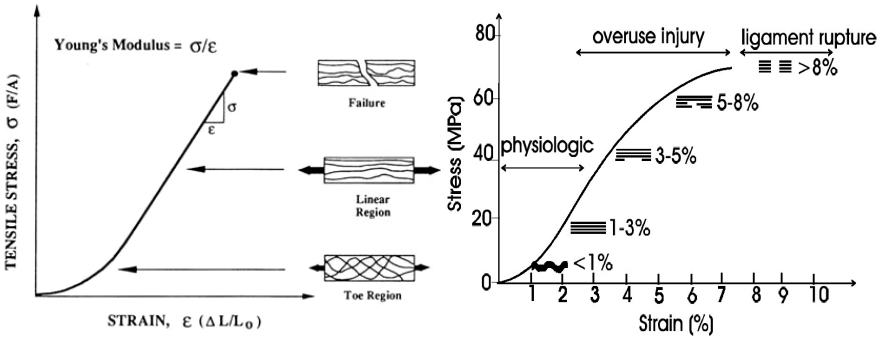

Fig. 2. Cartilage stress-strain curve (adapted from [7]), and Ligament stress-strain relationship. (modified from [8]). Young's modulus is defined by the slope of the linear region.

2.3 Ligament

Although significant advances have been made in the biology, biochemistry, and mechanics of soft tissue biomechanics, there is limited information available on in-vivo tissue mechanical characteristics and behavior. Experimental works, like the one of Stewart et al. [9] on ligaments of the hip joint capsule, bring important information that reveals the structural irregularity of that tissue. However, without accurate values of in-vivo information, such extrapolations from human – and also animal – insitu bone-ligament-bone testing to the function of intact human ligaments can not be made confidently. Currently, we know that ligaments are composite, anisotropic structures exhibiting non-linear time and history-dependent viscoelastic properties. Described in this section are the mechanical behavior of ligamentous tissue, the physiological origin of this behavior, and the implications of such properties to ligament function during normal joint motion.

The force-elongation curve represents rather structural properties of the tissues. Material properties, in turn, are more generally expressed in terms of a stress-strain relationship. See Fig. 2 for stress-strain relationship of ligament.

Ligaments have characteristics of strain rate sensitivity, stress relaxation, creep, and hysteresis. They exhibit significant time- and history-dependent viscoelastic properties. Time-dependent behavior means that, during daily activities, ligaments are subjected to a variety of load conditions that affect their mechanical properties. For example, they become softer and less resistant after some minutes of running, returning to normal hardness when the exercise is interrupted. History-dependency, in turn, means that frequent intense activities will change the tissue properties in a medium

term basis. For example, the ligaments of an athlete, after 6 months of daily training, will become softer and thus more adapted to the intense exercise, even when he is not training. In the same way, if the activities are interrupted for some months, the ligament properties will go back to normal levels. Ligaments are also temperature and age sensitive.

2.4 Conclusion

Biological tissues are materials of a very complex behavior. So the harder (bone) as the softer ones (cartilage and ligament) present non-linear mechanical properties that vary from sample to sample, are dependent on structure and composition, and are time and history dependent. As a consequence of such wide set of variants, existent measured properties are not reliable and just barely describe the general behavior of these materials. Despite of that, specific situations can be delimited in which we are able to predict behavior from a reduced set of input parameter values. One of these situations is the linear elastic deformation of soft bio-tissues. Here is where this work puts its focus.

3 Deformation Model

Approaches for modeling object deformation range from non-physical methods to methods based on continuum mechanics [10]. In this section, we focus on physically based approaches specifically used for modeling soft tissues. In this category, we present the two widest used, the classical mass-spring systems and finite element methods, and also our approach. Other physically based methods used to model deformable objects, like implicit surfaces and particles systems are not considered here.

3.1 Related Work

Mass-spring systems. Mass-spring is a physically based technique that has been widely and effectively used for modeling deformable objects. An object is modeled as a collection of point masses connected by springs in a lattice structure. Springs connecting point masses exert forces on neighboring points when a mass is displaced from its rest position.

Mass-spring systems have been widely used in facial animation. Terzopoulos and Waters used a three-layers mesh of mass points associated to three anatomically distinct layers of facial tissue (dermis, subcutaneous fatty tissue, and muscle) [11]. To improve realism, Lee et al. added further constraints to prevent penetrations between soft tissues and bone [12]. In biomechanical modeling, mass-spring systems were used by Nedel [13] to simulate muscle deformation. Muscles were represented at two levels: action lines and muscle shape. This shape was deformed using a mass-spring mesh. Aubel [14] used a similar approach with a multi-layered model based on

physiological and anatomical considerations. Bourguignon and Cani [15] proposed a model offering control of the isotropy or anisotropy of elastic material. The basic idea of their approach is to let the user define, everywhere in the object, mechanical characteristics of the material along a given number of axes corresponding to orientation of interest. All internal forces will be acting along these axes instead of acting along the mesh edges. Mass spring systems have also been used for cloth motion [16] and surgical simulation [17].

Mass-spring models are easy to construct, and both interactive and real-time simulations of mass-spring systems are possible even with desktop systems. Another well-known advantage is their ability to handle both large displacements and large deformations. However, mass-spring systems have some drawbacks. Since the model is tuned through its spring constants, good values for these constants are not always easy to derive from measured material properties. Furthermore, it is difficult to express certain constraints (like incompressibility and anisotropy) in a natural way. Another problem occurs when spring constants are large. Such large constants are used to model nearly rigid objects, or model non-penetration between deformable objects. This problem is referred as “stiffness”. Stiff systems are problematic because of their poor stability, which requires small time steps for numerical integration resulting in slow simulation [10].

Finite Elements Method. Whereas mass-spring models start with a discrete object model, more accurate physical models consider deformable objects as a continuum: solid bodies with mass and energies distributed throughout. Though models can be discrete or continuous, the method used for solving it is discrete. Finite element method is used to find an approximation for a continuous function that satisfies some equilibrium expression. In FEM, the continuum (object) is divided into elements joined at discrete node points. A function that solves the equilibrium equation is found for each element.

The basic steps in using FEM to compute object deformations are [10]:

1. Derive an equilibrium equation from the potential energy equation of the deformable system in terms of material displacement over the continuum.
2. Select the appropriate finite elements (generally, tetrahedra) and corresponding interpolation functions for the problem. Subdivide the object into elements.
3. For each element, re-express the components of the equilibrium equation in terms of the interpolation function and the element’s node displacements.
4. Combine the set of equilibrium equations for all the elements in the object into a single system. Solve the system for the node displacement over the whole object.
5. Use the node displacements and the interpolation functions of a particular element to calculate displacements or other quantities of interest (such as internal stress or strain) for points within the element.

Debunne et al. used a space and time adaptive level of detail, in combination with a large displacement strain tensor formulation [18]. To solve the system, explicit FEM was used where each element is solved independently through a local approximation, which reduces computational time. Hirota et al. [19] used FEM in simulation of mechanical contact between nonlinearly elastic objects. The mechanical system used as a case study was the Visible Human right knee joint and some of its surrounding bones,

muscles, tendons and skin. The approach relied on a novel penalty finite element formulation based on the concept of material depth to compute skin, tendons and muscles deformation. To achieve real-time deformation, reducing computing time is necessary. Bro-Nielsen and Cotin studied this problem using a condensation technique [20]. With this method, the computation time required for the deformation of a volumetric model can be reduced to the computation time of a model only involving the surface nodes of the mesh. The Boundary Element Method (BEM), used by James and Pai [21] to attain interactive speeds and accuracy at the same time for linear deformation, is also based on the FEM. The difference is that the BEM considers only the elements on the surface and use precomputed Green's functions that are combined later in real-time. Drawbacks of this method are that material properties must be homogeneous through all modeled object, and it is only suitable for surface-based applications.

FEM provide a more realistic simulation than mass-spring methods but are computationally less efficient. In addition, the linear elastic theory used to derive the potential energy equation assumes small deformation of the object, which is true for materials such as metal. However, for soft biological material, objects dimensions can deform in large proportions so that the small deformation assumption no longer holds. Because of this change, the amount of computation required at each time is greatly increased.

3.2 Molecules-based System

Our approach to model soft tissues is presented in this section. It is based on a work of Jansson et al. [2] that has been used in computer-aided design. Their work exploits a generalized mass-spring model – which they call molecular model – where mass points are, in fact, spherical mass regions called molecules. Elastic forces are then established between molecules by a spring-like connection. In the present work we aim at integrating properties of materials to define the stiffness of such spring-like connections.

The Force Model. The model is described by two sets of elements: *E*, a set of spherical elements (molecules), and *C*, a set of connections between the elements in *E* (Eq. 1).

$$E = \{e_1, e_2, \cdots e_n\}; C = \{C_{e_1}, C_{e_2}, \cdots C_{e_n}\}; C_{e_i} = \{c_1, c_2, \cdots c_m\} \quad (1)$$

The model's behavior is determined by the forces produced on each element of *E* by each connection of *C* and some external forces.

$$\vec{F}_e = \vec{F}_G + \vec{F}_L + \vec{F}_C + \vec{F}_{collisions} \quad (2)$$

, where:

F_G: gravity;
F_L: ambient viscous friction;
F_C: connection elastic forces, see [2] for more details.

3.3 Setting up springs stiffness

The rheological standard to define the elasticity of a material is Young's modulus. Young's modulus is a property of a material, not of an object. So it is independent of the object's shape. However, when you discretize an object by a set of springs, the stiffness of every spring must be proportional to the fraction of the volume of the object it represents.

Towards a generic method to calculate all spring constants we tested a number of hypotheses. These tests have been done on an implementation of our model where objects were deformed due to a homogenously distributed force on one of their faces. To verify the correspondence between the deformation obtained with our model and the deformation that the object should undergo with respect to its Young's modulus we used the following relation:

$$E = \frac{F \cdot l_0}{\Delta l \cdot A}, \tag{3}$$

where E is the Young's modulus, F is the applied force, Δl is the object's elongation, l_0 is the length of the object in rest conditions, and A is the cross-sectional area of the object. So, we started by the simplest linear topology case and went through many variations until the generic random topology. Section 4 and conclusions compare the effectiveness of every method presented below.

Linear case. In the case where all springs produce force in only one direction and one wants to measure elasticity in the same direction, one can easily calculate the constant k of the springs directly from the geometrical information of the object and the Young's modulus of its material. This is done using Eq. 4. The problem of this very specific case is that its rectangular topology does not allow the construction of stable objects in two or three dimensions (Fig. 3). To overcome this limitation, we propose two strategies. The first using tetrahedral discretization and the second including diagonal springs to the rectangular topology. Both methods allow us to obtain stable objects. However, diagonal springs can make the number of springs grows up to $(n^2 - n) / 2$, where n is the number of molecules. This increases computation time.

$$k = \frac{EA}{l_0} \tag{4}$$

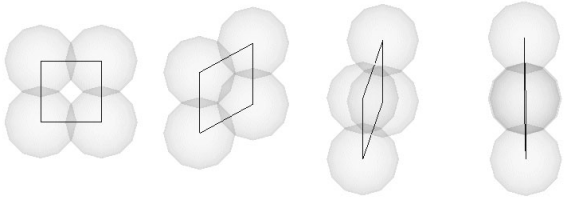

Fig. 3. These four situations are stable states with a rectangular topology. These and many other different relative positions between spheres are allowed for the same elongation of springs.

Tetrahedral regions. A straightforward path in order to reach object stability is creating a tetrahedral mesh of springs. Gelder [22] presented a method to calculate stiffness for elastic edges of triangular meshes. His approach is based on the area of the triangles formed by the edge. He also proposed the extension of this approach to 3D, where volumes of neighboring tetrahedra are used to calculate the k for an edge. The main drawback of this method is that it only works if the mesh of springs has a tetrahedral topology. k is calculated as shown in Eq. 5, where E is the Young's Modulus, T_e is a tetrahedron incident upon c, and c is the edge to which we are calculating k.

$$k_c = \frac{E\sum_e vol(T_e)}{|c|^2} \tag{5}$$

Diagonal springs. In order to avoid tetrahedral meshes we have chosen to create diagonal spring connections in every face of a rectangular mesh of springs, as shown in Fig. 4, or yet, create also diagonals of parallelepipeds (Fig. 5). It offered the desired result but gave rise to a difficulty in terms of computing spring constants.

If we use the standard linear method to compute them, the diagonal springs will produce an extra force to linear movement that will causes elongation of the whole object to be shorter than expected. The object will become abnormally stiffer, and to avoid this some method should be developed to reduce springs k's. The straightforward solution is to divide all linearly calculated k's by a constant C. We tested arbitrary values to C and concluded that even for the same topology, when other parameters change, such constant must change to preserve the same elasticity.

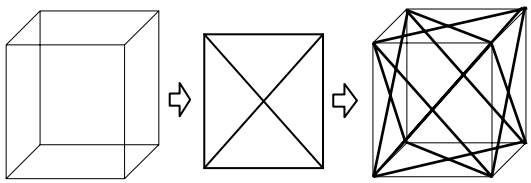

Fig. 4. Diagonals of faces.

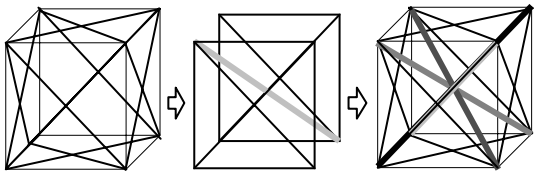

Fig. 5. Diagonals of parallelepipeds.

Angles solution. As we do not want to work manually to find which constant C best fits each new object or topology, we implemented a method that automatically calculate new k's based on diagonal's angles.

Bringing the problem to 2D to make explanation easier, we see that force produced in vertical direction is increased by diagonals springs according to the angles between them. As we have right triangles in this topology, the relationship between a vertical connection and a diagonal one is proportional to cosine and the final k is given by the relation:

$$k_f = k_0 \cos_0 + k_1 \cos_1 + ... + k_n \cos_n \quad , \tag{6}$$

where index *0* represents the connection to which we are calculating k, and indexes *1* to n the connections that share an extremity with *0*. cos_i is the cosine of the angle between connections *0* and i. Considering a homogeneous object, all k_i/l_i (where l_i is the length of connection i) are equal. So, from this and Eq. 6 we deduce:

$$k = \frac{k_f}{(l_0 + l_1 \cos_1 + ... + l_n \cos_n)} \cdot \tag{7}$$

This approximates the actual value of k. However, angles change along simulation and should be calculated for every iteration, which causes cost increase. Even worse, the right triangles deform along simulation becoming arbitrary triangles, which invalidates this method.

General case. As we have just seen, during deformation the molecules may change their positions so that diagonals' angles are no longer right angles. Besides, arbitrary initial topologies may have some angles that are not right angles from the beginning. To handle these cases we have developed a novel method to calculate spring constants. It is a statistical method inspired on general concepts of Quantum Mechanics that heuristically estimates new values for k from the number of connections around a molecule. As the number of connections of a molecule increases, smaller is the portion of the object's volume that each connection represents, and its spring constant must be smaller too. So, though we do not calculate exactly the volume represented by a connection, we can probabilistically guess which topological case we have, just counting how many connections share a molecule. Fig. 6 illustrates some typical 2D situations.

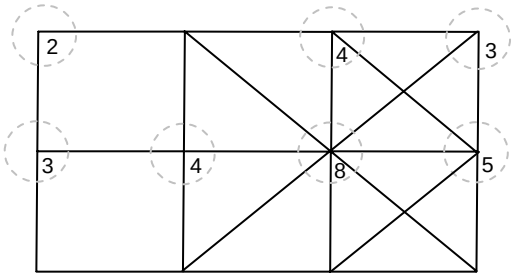

Fig. 6. Different situations and their numbers of connections.

We considered the 3D case and the diagonal on faces topology, and stated the following algorithm to calculate Hooke's constant for every connection of an object. This algorithm should present better results when larger and larger numbers of molecules are involved. It would happen because statistically, the finer the sampling the smaller the error.

Algorithm that calculates Hooke's constant based in our statistical method.

```
N1 = number of connections of molecule 1
N2 = number of connections of molecule 2
D1; //estimated num. of directions among conn. of m. 1
D2; //estimated num. of directions among conn. of m. 2
if N1 < 8
   D1 = N1
else if ( N1 >= 9 ) AND ( N1 < 12 )
   D1 = N1 - 1
else if ( N1 >= 13 ) AND ( N1 < 20 )
   D1 = N1 - 4
else if N1 >= 20
   D1 = N1 / 2
end
if N2 < 8
   D2 = N2
else if ( N2 >= 9 ) AND ( N2 < 12 )
   D2 = N2 - 1
else if ( N2 >= 13 ) AND ( N2 < 20 )
   D2 = N2 - 4
else if N2 >= 20
   D2 = N2 / 2
end
area1 = ( 2 * cross-sectional area ) / D1
area2 = ( 2 * cross-sectional area ) / D2
hooke = ( Youngs Modulus of molecule 1 * area1
        + Youngs Modulus of molecule 2 * area2 )
        / ( 2 * nominal distance )
```

Iterative Solution. The division by a constant approach mentioned earlier can be extended by automatically calculating the value of *C* according to the obtained deformation. The elongation in a specified dimension of an object can be applied in Eq. 3 to verify, for a given force, what is the effective Young's modulus (*E*) of the object at each time step. Doing that iteratively in the simulation loop we can minimize the difference between the obtained and the specified *E* changing the value of *C* according to it.

4 EXPERIMENTS

We implemented the model described in Sect. 3.3 in the form of a framework that will be used in a future work to develop medical applications. The code has been written in C++ on PC platform. In this implementation the forces are integrated along time to produce new molecules positions in a static simulation.

4.1 Test Scenarios

A number of experiences have been performed to test the validity of the hypotheses of Sect. 3.3. Four deformable objects have been created which represent the same volume in the space (Fig. 7). Though they do not have exactly the same volume, the regions considered here have exactly the same vertical length and nearly the same cross sectional area. The vertical length of the considered volume, in the initial state is equal to 15 mm and its cross-sectional area is around 9 cm^2. The superior extremity of the objects is fixed and a tension force of 1 N is applied on the inferior extremity. The elasticity of the material is specified as 5000 N/m^2 (= 5 kPa).

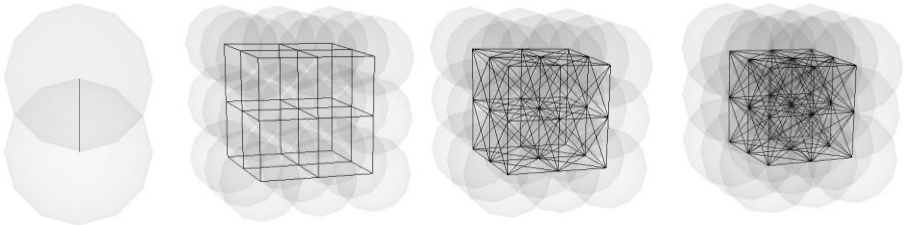

(a) **2 molecules** **1 connection**

(b) **27 molecules** **54 connections**

(c) **27 molecules** **126 connections**

(d) **27 molecules** **158 connections**

Fig. 7. Scenarios being studied.

For each object we computed all methods to calculate k presented in Sect. 3.3. Table 1 compares the results obtained for Young's modulus when each method is used for calculation of *k*. The method based on tetrahedral regions has not been implemented here; we rely on the work of Gelder [22]. Later, to inspect the behavior of the methods when the number of molecules grows drastically, we created the situation of Fig. 8 where 1000 molecules and 7560 connections represent a volume of approximately 1 m^3. The vertical length of the considered volume, in the initial state is equal to 86 cm and its cross-sectional area is 1 m^2. One extremity of the object is fixed and a tension force of 1000 N is applied on the other one. The elasticity of the material is specified as 10^5 N/m2 (= 100 kPa). The obtained results are in Table 2.

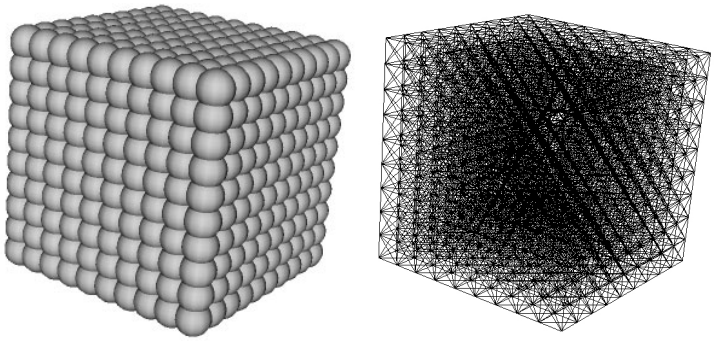

Fig. 8. Test with an increased number of molecules and connections. 1000 molecules and 7560 connections are used to model this box.

Table 1. Resultant elasticity obtained with the different methods for the 4 cases of Fig. 7. Shaded cells indicate correct values or with a small acceptable error.

Method	Young's Modulus (N/m^2) / error (%)							
	(a)		(b)		(c)		(d)	
Linear case	4'994	0.12	4'996	0.08	12'465	149.30	20'678	313.56
Statistical	10'004	100.08	6'098	21.96	3'637	27.26	4'904	1.92
Angles	4'997	0.06	5'000	0.00	4'916	1.68	5'903	18.06
Angles (update)	4'999	0.02	4'996	0.08	11'550	131.00	18'621	272.42
Iterative	5'000	0.00	5'000	0.00	5'000	0.00	5'000	0.00

Table 2. Tension tests results for a cube of elasticity expected to be 10^5 N/m^2.

Method	Elongation (mm)	Young's Modulus (N/m^2)	Error (%)
Linear case	2.300	373'913	274
Statistical method	11.384	75'544	24
Angles	5.890	146'010	46
k / 3.75	8.603	100'000	0
Iterative	8.600	100'000	0

5 Discussion and Conclusions

None of the methods tested here works unconditionally for any case. Though the iterative solution provided our best results so far, it requires a strategy to specify the direction in which E will be measured and some cases may present numerical instabilities, which may disturb convergence. Only after new tests we can use it as a generic solution.

Standard method always works if mesh topology is rectangular, angles method if the diagonals form right triangles, and statistical method approximates the correct value in any case but usually gave objects softer than we expected. Both angles and statistical method can still be improved and we will keep working in this direction. We will also consider implementing tetrahedral method to apply it onto an intermediate tetrahedral mesh that can be constructed from arbitrary meshes, and then use the calculated values into the same arbitrary mesh. All our tests have been done applying tensile forces, but others, like shear test, must be done in order to validate a method for our purposes. Even if a spring configuration gives good results in tensile tests, we cannot affirm shear tests will also be correct. Finally, many important properties of tissues have not been taken into consideration in this work, like anisotropy and viscosity of tissues. Once these features become part of our deformation model, properties of materials will change over time, and any method used to configure our spring-like connections must take this factor into account to properly update all parameters during simulation.

REFERENCES

1. Maciel, A., Boulic, R., Thalmann, D. *Towards a Parameterization Method for Virtual Soft Tissues based on Properties of Biological Tissue* In. 5th IFAC 2003 Symposium on Modelling and Control in Biomedical Systems, Melbourne (Australia). Elsevier (to appear).
2. Jansson, J. and Vergeest, J. S. M. A discrete mechanics model for deformable bodies. Computer-Aided Design. Amsterdam (2002).
3. Fung, Y-C. *Stress-Strain History Relations of Soft Tissues in Simple Elongation*. In Biomechanics: Its foundations and Objectives, Prentice Hall, Englewood-Cliffs (1972).
4. Fung, Y-C. *Biomechanics: Mechanical Properties of Living Tissues.* Second Edition, Springer-Verlag, New York (1993).
5. Washington University Departments web site. *Bone Structure.* Available at: http://depts.washington.edu/bonebio/bonAbout/structure.html.
6. Mow, V. C. and Hayes, W. C. *Basic Orthopaedic Biomechanics*. Second Edition. Lippincott-Raven Publishers (1997).
7. Mow V. C. et al. *Structure and Function of Articular Cartilage and Meniscus.* Basic Orthopaedic Biomechanics, Raven Press, New York (1991).
8. Butler, D.L. et al. *Biomechanics of ligaments and tendons.* Exercise and Sports Science Reviews, 6, 125-181 (1984).
9. Stewart, K. J. et al. *Spatial distribution of hip capsule structural and material properties*. In: Journal of Biomechanics. n. 35, pp. 1491-1498. Elsevier (2002).
10. Gibson, S. F. F. and Mirtich, B. A *Survey of Deformable Modeling in Computer Graphics.* Technical Report No. TR-97-19, Mitsubishi Electric Research Lab., Cambridge, (1997).
11. Terzopoulos, D. and Waters, K. *Physically-Based Facial Modeling, Analysis, and Animation*. The Journal of Visualization and Computer Animation, Vol.1, pp. 73-80, (Dec. 1990).
12. Lee, Y. and Terzopoulos D. *Realistic Modeling for Facial Animation*. Proceedings of SIGGRAPH 95, Computer Graphics Proceedings, Annual Conference Series, pp. 55-62, Los Angeles (1995).
13. Nedel, L. P. and Thalmann, D. *Real Time Muscle Deformations Using Mass-Spring Systems*. Computer Graphics International 1998, pp. 156-165, Hannover (1998).
14. Aubel, A. and Thalmann, D. *Interactive Modeling of Human Musculature.* Computer Animation 2001, Seoul (2001).
15. Bourguignon, D. and Cani, M-P. *Controlling Anisotropy in Mass-Spring Systems.* Computer Animation and Simulation 2000, pp. 113-123, Interlaken (2000).
16. Baraff, D. and Witkin, A. *Large Steps in Cloth Simulation.* Proceedings of ACM SIGGRAPH'98, ACM Press (1998), pp. 43-54.
17. Brown, J. et al. *Real-Time Simulation of Deformable Objects: Tools and Applications.* In Computer Animation 2001, Seoul (2001).
18. Debunne, G. et al. *Dynamic Real-Time Deformations Using Space & Time Adaptive Sampling.* Proceedings of SIGGRAPH 2001, pp. 31-36, Los Angeles (USA), 2001.
19. Hirota, G. et al. *An Implicit Finite Element Method for Elastic Solids in Contact*. In Computer Animation 2001, Seoul (2001).
20. Bro-Nielsen, M. and Cotin, S. *Real-time Volumetric Deformable Models for Surgery Simulation using Finite Elements and Condensation.* Computer Graphics Forum (Eurographics'96), 15(3), pp. 57-66 (1996).
21. James, D. L. and Pai, D. K. *ArtDefo – Accurate Real Time Deformable Objects*. Proceedings of SIGGRAPH 99, Computer Graphics Proceedings, Annual Conference Series, pp. 65-72, Los Angeles (1999).
22. Gelder, A. *Aproximate Simulation of Elastic Membranes by Triangulated Spring Meshes.* In: Journal of Graphics Tools. v. 3, n. 2, pp. 21-42. A. K. Peters, Ltd. Natick (1998).